Hydrodynamic Aspects of Waste Discharge

MARSHALL P. TULIN*
Hydronautics, Incorporated, Laurel, Md.

AND

JOSEF SHWARTZ†
Hydronautics-Israel, Ltd., Rehovoth, Israel

Here we discuss in terms of several specific examples, some important hydrodynamic effects which arise in connection with the discharge of waste, including effects which are due to buoyancy and stratification. Specific models of important discharge flows which are discussed in some detail are: the rise of a hot chimney plume into a stable stratified atmosphere; and the spreading of an underwater thermal discharge along the free surface of a moving body of water. The plume has been much discussed previously, and the present understanding is reviewed. The spreading of a thermal discharge, however, does not seem to have been previously treated in detail. Plume motions in a stable stratified atmosphere involve different regimes of motion. The ideal bent-over and rising chimney plume comprises a self-similar, self-convecting motion for which predictions may be made with the aid of conservation laws. These laws are discussed together with explicit results derived from their application; comparisons are made with full-scale data. When buoyant material is discharged into a shallow stream, it rises to the free surface where it spreads. A model of the spreading mechanism is postulated, an asymptotic (thin layer) theory is derived, and predictions of the spreading behavior are made. The possible influences of turbulent mixing due to initial and maintained sources of turbulence are discussed, and a comparison is made with limited full-scale data.

Nomenclature

a = (I)‡ density gradient in surrounding fluid, $a = 1/\rho_e d\rho_e/dz$
a_1,a_2,a_3,a_4 = (II)‡ distribution coefficients
A = (I) coefficient relating rise and horizontal distance, Eq. (9)
B = (I) coefficient in Brigg's relation, Eq. (2)
B = (II) turbulent entrainment coefficient for spreading mass, excluding head entrainment
B' = (II) head entrainment coefficient
C = (II) half-width of cross section of density current
c_p = (I) concentration of species p
C_D = (I) energy dissipation coefficient
C_D = (II) turbulent energy dissipation coefficient
C_D' = (II) head drag coefficient
D = (I) energy dissipation parameter, $D = C_D/\beta K$
D_h = (I) drag acting on head of density current
F = (I) chimney flux
F = (II) froude number related to density current, $F = U/(\Delta\rho/\rho_e \cdot g \cdot h(o))^{1/2}$
F_p = (I) flux of species p
g = (I,II) acceleration of gravity
G = (I) initial buoyancy parameter, $G = -(\Delta\rho/\rho_e)_o$
h = (II) local vertical thickness of density current
$h(o)$ = (II) thickness behind head of steady density current, Fig. 7
$h(c)$ = (II) thickness of density current at head
k = (I) virtual potential energy coefficient
K = (I) virtual kinetic energy coefficient
l = (I) buoyancy scaling length, $l = F/U^3$
δm_1 = (II) excess mass of spreading fluid
M = (I) initial momentum parameter, $M = w_o^2/gz_o$
n = (I) dissipation parameter, $n = 2(1 + D)$
r = (I) effective cross-sectional radius of vortex pair
S = (I) density stratification parameter, $S = az_o/3$
t = (I,II) time
t_v = (I) Vaissala period (of internal waves), $t_v = 2\pi/(ag)^{1/2}$
u = (II) horizontal velocity within density current
U = (I,II) horizontal mean velocity of external stream
$\bar{U}$ = (I) $U/(gz_o)^{1/2}$
v' = (II) turbulence intensity within density current
v_o = (II) initial characteristic turbulence intensity
V = (II) density current volume
w = (I) vertical mean velocity
x = (I) horizontal distance
x = (II) lateral distance
$\bar{x}$ = (I) x/z_o
y = (II) vertical distance
z = (I) vertical distance
$\alpha,\beta,\gamma,\delta$ = (II) exponents, Eq. (32)
β = (I) entrainment coefficient, Eq. (1)
δ^* = (II) displacement thickness of the wake due to head breaking
κ = (I) $2k/K$
η = (II) nondimensional lateral distance, $\eta = x/c$
ρ = (I,II) fluid density
$\Delta\rho$ = (I,II) density difference, $\Delta\rho = \rho_i - \rho_e$

Subscripts

i = internal
e = external
o = initial values

Superscripts

$*$ = (II) time dependent, characteristic quantities
barred quantities = (I,II) nondimensionalized

Presented as Paper 70-755 at the AIAA 3rd Fluid and Plasma Dynamics Conference, Los Angeles, Calif, June 29–July 1, 1970; submitted September 18, 1970; revision received September 27, 1971.

* Technical Director.

† Principal Research Scientist; and Senior Lecturer, The Technion, Haifa, Israel. Member AIAA

‡ I refers to Sec. I—Chimney Plumes, and II refers to Sec. II—Thermal Discharge in Streams.

I. Chimney Plumes

Introduction

THE ultimate fate of hot waste gases and particulate matter emitted from chimney stacks depends upon a variety of factors. These include: the diameter, tempera-

ture, and initial velocity of the exhaust; meteorological conditions such as the steady and fluctuating wind distribution; and density gradients in the atmosphere.

During the life time of a plume, measured in terms of transit time downwind from the stack, distinct regimes may be recognized in which different hydrodynamic phenomena govern. In the case of a plume emitted into a stable stratified and gusty wind field, at least the following regimes (sometimes overlapping) may be identified: bending over; buoyant rise; fall and collapse; gust meandering and dispersion.

Gases exhausted into a cross wind are swept by the wind and bent over after traveling a relatively short distance upward, usually only 2–5 stack diameters. The gases within the bent-over and nearly horizontal plume are moving essentially with the wind in the downwind direction, while a transverse cross section or slice of the plume may be observed to be moving vertically. These transverse slices resemble very closely, both in appearance and in their characteristics, an equivalent section of a two-dimensional turbulent vortex pair (Fig. 1). This vortex-pair is originally created in the interaction between the vertical exhaust and the wind which bends it over (see Keffer and Baines[1] and Keffer[2]). Subsequently, the vorticity within the plume slices is modified as these slices rise under the influence of their initial momentum and of their excess buoyancy. The latter is preserved in the motion and eventually dominates it.

It is naturally of interest to understand the way in which the various factors previously mentioned enter into determining the rate at which the plume rises and disperses, the maximum altitude reached by the plume, and the distance downwind at which it is reached. Although the real situation is highly variable and complex in terms of the factors at work, rather simple analyses of a fluid mechanical nature prove to yield a great deal of useful information and insight. It is our purpose here briefly to review the theory and its implications, with an emphasis on the case of plume motion in a stable stratified atmosphere without gusts. The present theory of chimney plumes may be said to have originated with Scorer,[3] who treated the case of the neutral atmosphere; it has been extended in recent times to motions in stratified atmospheres.[4,5] It will not be possible here to give adequate reference to all of the contributions to this subject.

Cross Flow Theory

To a good approximation, the vertical rise of a plume in a steady horizontal wind (velocity U) can be analyzed in terms of a two-dimensional unsteady motion in the cross flow plane upon substitution of the downwind distance x/U by the time t. This is, of course, the same procedure introduced into aerodynamics by Max Munk, and used with such great success in the analysis of the lifting flow about slender bodies and low-aspect ratio wings. It depends for its success on the fact that changes in the cross flow occur relatively slowly in the downwind direction.

In distinction to the usual aerodynamic case, the shape of the plume in time (its diameter, for example) is not known in advance but must be determined. In addition, the motion is essentially turbulent and very much dependent on the turbulent entrainment of ambient fluid into it. The most general analyses which have been made are based on the assumption of self-similarity and of a linear entrainment law, both first introduced by Morton, Taylor and Turner[6] in their analysis of turbulent gravitational convection from maintained and instantaneous sources. Self-similarity implies that the dimensions of the rising mass and the associated velocities and densities at two different points in space or time, whether within or external to the vortex pair, can usually be reduced from one to the other upon normalization by appropriate (characteristic) length, velocity and density scales. The theory which results from these assumptions must be regarded as provisional, since it is doubtful, at least, that self-similarity really pertains in the case of most interesting flows.

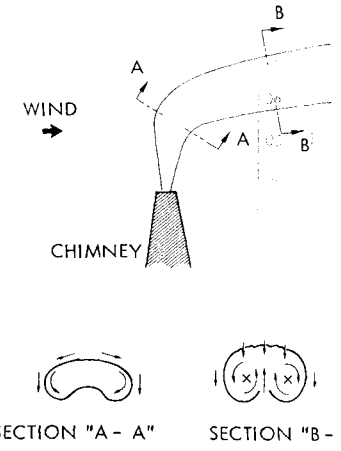

Fig. 1 Characteristic cross sections of a smoke plume.

The characteristic length, velocity, and density scales may be determined with the aid of a like number of independent conservation laws. Following Morton, Taylor and Turner, these are usually for volume, buoyancy (or mass), and momentum. In the present example, however, we introduce below energy conservation, e.g., Eq. (3) in place of momentum, following Tulin and Shwartz.[7] A similar analysis, utilizing momentum conservation has been given by Hoult, et al.[4] The coupled differential equations for the density deficit and the vertical velocity are readily given analytical solution, although the trajectories themselves must be determined numerically.

The conservation equations used in Ref. 7 by Tulin and Shwartz in the case of a two-dimensional vortex pair rising in a stratified atmosphere are written:

$$(d/dt)(\pi r^2) = \beta w(2\pi r) \tag{1}$$

$$(d/dt)(\pi r^2 \rho_i) = \beta w(2\pi r)\rho_e \tag{2}$$

$$d/dt[(K/2)\rho_i w^2 r^2 + k(\rho_i - \rho_e)gzr^2] = -C_D \rho_i w^3 r \tag{3}$$

where r (radius), w (vertical velocity), ρ_i (internal density) and z (vertical distance), are all time dependent, while ρ_e (external density) varies with height z depending on the stratification of the surrounding fluid; K and k are the virtual kinetic and potential energy coefficients, respectively, and β is an entrainment coefficient. The above set of equations is complete when we add the kinematic relationship $w = dz/dt$. Upon differentiating Eq. (1), Eq. (3) and introducing the usual Boussinesq approximation ($\rho_i/\rho_e \approx 1$) where appropriate, these may be put in the form:

$$dr/dz = \beta \tag{4}$$

$$d/dz(\Delta\rho/\rho_e) + 2/z(\Delta\rho/\rho_e) = a \tag{5}$$

$$zdw^2/dz + 2(1 + C_D/\beta K)w^2 + 2kg/K(\Delta\rho/\rho_e + az)z = 0 \tag{6}$$

where a is the normalized density gradient of the surrounding fluid and $\Delta\rho = \rho_i - \rho_e$.

Solutions, in terms of suitable nondimensional parameters, are:

$$\Delta\rho/\rho_e = S(z/z_o) - (G + S)(z_o/z)^2 \tag{7}$$

$$\frac{w^2}{gz_0} = \left[M - \frac{\kappa}{1+2D}G + \left(\frac{\kappa}{1+D/2} - \frac{\kappa}{1+2D}\right)S\right] \times \left(\frac{z_o}{z}\right)^n + \frac{\kappa}{(1+2D)}(G+S)\left(\frac{z_o}{z}\right) - \left(\frac{\kappa}{1+D/2}\right)S\left(\frac{z}{z_o}\right)^2 \tag{8}$$

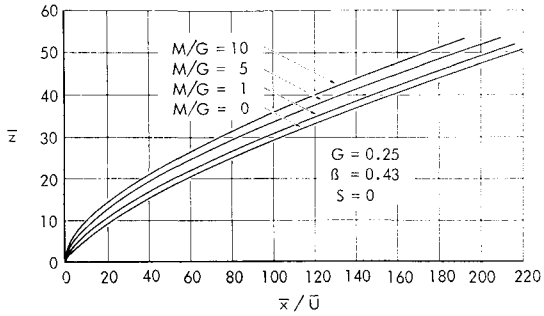

Fig. 2 The effect of smoke plume's initial vertical velocity on its trajectory, Eq. (10).

where

$$\kappa = 2k/K; \quad D = C_D/\beta K; \quad n = 2(1 + D)$$

$$M = w_o^2/gz_o; \quad G = -\left(\frac{\Delta\rho}{\rho_e}\right)_o; \quad S = az_o/3$$

The latter three parameters characterize both the rising mass and its environment; M being a measure of the initial momentum of the rising mass, G of its initial buoyancy, and S of the ambient fluid stratification.

The initial buoyancy of the plume is usually measured in terms of the plume buoyancy flux at the stack exit, πF, which is the product of the stack heat flux and g, divided by the product of density, heat capacity, and absolute temperature of the atmosphere at the stack exit height. The parameter G may be determined from F according to the relation,

$$G = F/r_o^2 Ug$$

Asymptotic Results, Neutral Atmosphere ($S = 0$)

In this case, the effects of buoyancy predominate after a long enough time, and,

$$\Delta\rho/\rho_e \sim -G(z_o/z)^2$$

$$w^2/gz_o \sim \kappa/(1 + 2D)\cdot Gz_o/z$$

The latter expression, when integrated leads to a trajectory:

$$z/z_o = [\kappa G/(1 + 2D)]^{1/3}(3\bar{x}/2U)^{2/3} \tag{9}$$

or

$$(z/l) \sim A(x/l)^{2/3}$$

where, $l = F/U^3$, a buoyancy scaling length commonly used in plume-rise analysis. The form of this trajectory was first predicted by Scorer[3] on the basis of dimensional arguments, later by Briggs,[8] in the same way, and still later determined with the aid of more detailed fluid mechanical analysis by Slawson and Csanady,[9] and Hoult et al.[4] These authors found $A = (3/2\beta^2)^{1/3}$ whereas the present analysis leads to:

$$A = \{9/4[\kappa/(1 + 2D)\beta^2]\}^{1/3}$$

When $\kappa = 1$, these results are consistent for $D \approx \frac{1}{4}$.

The theoretical trajectory, Eq. (9), is in good agreement with recorded plume rise in a neutral atmosphere and Slawson and Csanady[9] found the best correlation for $A = 2.3$, suggesting $\beta = 0.35$ according to their own theory. Briggs suggested $A = 2.0$. It would be highly desirable to carry out a good correlation of A and β on the basis of field observations.

Increasing Exhaust Velocity ($S = 0$)

How effective is increased exhaust velocity in raising the plume trajectory? We have calculated the trajectory for various values of M/G, upon the assumptions: $\kappa = 1$; $D = 0$; it is:

$$\left[\bar{z} + 2\left(1 - \frac{M}{G}\right)\right]\left[\bar{z} - \left(1 - \frac{M}{G}\right)\right]^{1/2} = \left(3 - \frac{M}{G}\right)\left(\frac{M}{G}\right)^{1/2} + \frac{3}{2}(G)^{1/2}\left(\frac{\bar{x}}{\bar{U}}\right) \tag{10}$$

which is shown plotted for some particular cases in Fig. 2. In terms of the nondimensional coordinates, $\bar{z}$ and $\bar{x}/\bar{U}$, an increased exhaust velocity, or M, has a relatively small effect on the rise, $\bar{z}$, of the plume, particularly where it is far removed from the stack. However, care must be exercised in the interpretation of this figure, since the actual height and lateral distance of the plume from the stack mouth depend also on the initial values for the plumes vertical motion, such as z_o, which may depend on the exhaust conditions, including the exhaust velocity.

Buoyant Plumes in a Stable Atmosphere

The plume density-deficit continually decreases as it rises and entrains ambient fluid. In rising into a continuously stratified atmosphere it eventually reaches an altitude where the surroundings possess the same density as the plume itself. As a result, its ultimate altitude becomes restricted. We have carried out systematic experiments on the rise of two-dimensional vortex pairs into a linearly stratified atmosphere. Their motion is probably similar to that of plume cross sections, even though the vortex pairs in our experiments were not buoyancy dominated. We observed that the trajectory of a vortex pair rising into a stable atmosphere can be divided into three regimes: rising; falling and collapse; lateral spreading. In the rising region the vortex pair moves vertically upward starting with some initial imposed velocity. This gradually decreases in rising, because of the entrainment of surrounding fluid. The buoyancy also declines continuously, eventually reversing its sign, causing a reversal in the motion. During the downward motion, the pair continues to entrain fluid, but less effectively than during the rising regime. While falling, the vortex pair tends to collapse. That is, under the action of gravimetric forces the width of the pair increases while its thickness decreases. The widening pair continues its fall past the level of neutral density, reaches a minimum in its descent and reverses again its direction of motion; it now spreads laterally. The complete trajectory is illustrated in Fig. 3, which relates to actual experimental observations of a vortex pair.

According to Tulin and Shwartz[7] the rising portion of the plume trajectory $\bar{z}$ in a stratified atmosphere may be estimated through integration of:

$$(d\bar{z}/d\bar{t})^2 = (G + S)\bar{z}^{-1} - S\bar{z}^2 - G\bar{z}^{-2} \tag{11}$$

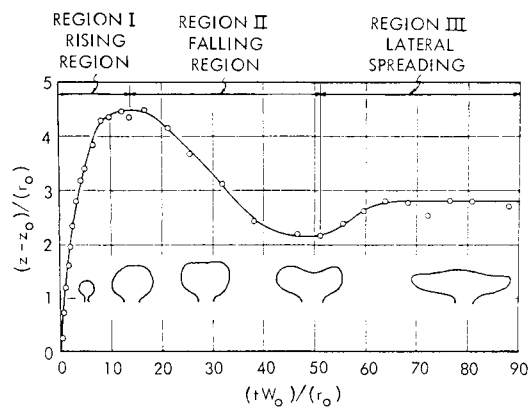

Fig. 3 The trajectory of a vortex pair in a stable density-stratified medium with its characteristic cross sections.

The numerical value of S as determined by the atmospheric conditions, is usually very small. In a neutrally stable adiabatic atmosphere, a and S are both zero. For an isothermal atmosphere, e.g., at 80°F, $a = 1 \times 10^{-5}$ ft^{-1}, and S is of order 10^{-4}. Some trajectories calculated according to Eq. (11) are shown as Fig. 4 for various values of S.

Estimates of maximum height of plume rise were made by Briggs[8] on the basis of dimensional considerations. Tulin and Shwartz[7] also provided an estimate based on the solution of Eq. (11) further simplified by assuming $\bar{z} \gg 1$. They both found

$$z_{\max} = B(F/agU)^{1/3} \tag{12}$$

where Briggs recommended a value $B = 2.6$ based on correlation with available field data. The latter authors found

$$B \approx (3/\beta^2)^{1/3} \tag{13}$$

which provides a value of 2.6 in the case $\beta = 0.42$. They also compared Eq. (11) with the recent observations of Bringfelt[10]; the results are shown in Fig. 5. The best correlation corresponds to a value $\beta = 0.48$.

The downstream distance at which the maximum plume height is reached was estimated by Tulin and Shwartz[7] according to theory to be

$$(x/l)z_{\max} = 1.1(3U^2/agl^2)^{1/2} \tag{14}$$

independent of β.

The downwind time required to reach this condition is $(t = x/U)$,

$$(t)_{z_{\max}} = \frac{1.1(3)^{1/2}}{(ag)^{1/2}} = \frac{1.9}{(ag)^{1/2}} \tag{15}$$

a simple result in very close agreement with our laboratory observations on vortex pairs rising in a wide range of stratified conditions, where a mean value of 1.7 was determined in the place of the constant 1.9 in Eq. (15).

The time to rise is thus scaled with the Vaissala time t_v of the atmosphere. This time, $t_v = 2\pi/(ag)^{1/2}$ is the fundamental period of internal wavelike motions which can occur on account of density stratifications, motions such as lee-waves in the atmosphere and internal waves in the ocean. The Vaissala time also scales the falling and collapse phenomena; Wu[11] has found experimentally that the time of collapse of a well-mixed region in stratified surroundings was $0.7t_v$. In an isothermal atmosphere, the Vaissala time is approximately 5 min.

Based on the previous discussion it can be understood that the effect of stratification is to flatten the plume in the horizontal plane at some altitude determined by atmospheric conditions. It can be estimated from Fig. 4 that over the likely range of atmospheric stabilities ($S = 4$–10×10^{-5}) which accompany temperatures rising with altitude, the range of heights at which the plume may find its equilibrium will be relatively small, $\bar{z} \sim 20$–30. At the same time, under the same conditions of stability the vertical component of

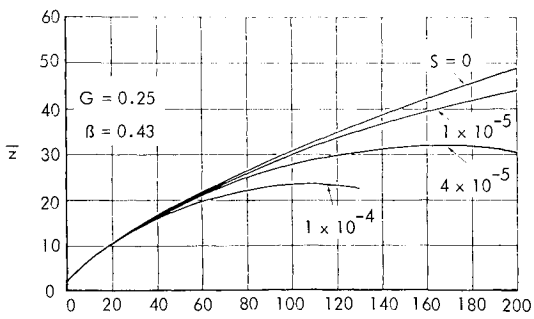

Fig. 4 The effect of atmospheric density-stratification on smoke plume trajectory, Eq. (11).

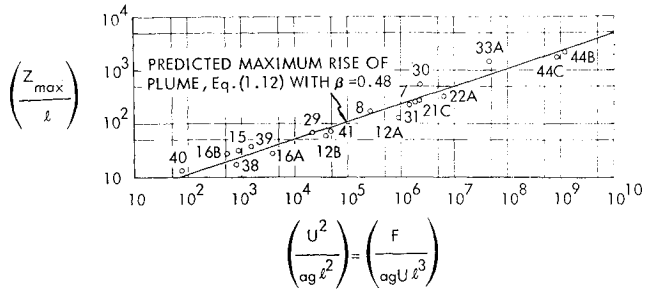

Fig. 5 The maximum rise of chimney plumes in a stratified atmosphere; comparison of field observations from Bringfelt (1968) with theory.

atmospheric turbulence will be suppressed if the wind speed is low enough. It is in this way that a smoke blanket at altitudes of several thousand feet may be created under conditions of moderate to strong stability and of sufficiently light winds.

Dilution

The emitted heat and waste materials are carried along in the bent-over plume and their mean concentration is continuously diluted due to enlargement of the plume cross section during its rise. The downstream flux of a given species p is conserved and equal to the emitted flux F_p

$$\pi r^2 c_p \cdot U = F_p \tag{16}$$

where c_p is the concentration. The assumptions underlying the simple conservation equations lead to $r = \beta z$, a virtual origin z_o. Consequently it may be shown, using the results previously discussed, especially Eq. (9), that in the case of plume rise in a homogeneous atmosphere

$$c_p = F_p U x^{-4/3}/F^{2/3}(\beta A)^2 \tag{17}$$

A similar result has been found by Tsang,[12] who also made a comparison with field measurements, showing fair agreement.

It is to be noted that the concentration decreases more rapidly in the plume than in the case of either a round jet emitted into a stationary fluid ($c_p \sim x^{-1}$) or a typical wake in a homogeneous fluid ($c_p \sim x^{-2/3}$).

The enlargement of the cross section by entrainment due to rise will be limited in a stable atmosphere. In this case, the concentration at the maximum height of rise is, using Eq. (12),

$$c_{p(z_{\max})} = [(ag)^{2/3}/U^{1/3}(\beta B)^2]F_p/F^{2/3} \tag{18}$$

illustrating further the unfavorable effect of stable conditions on the dispersion of emitted materials.

II. Thermal Discharge in Streams

Introduction

Let us turn our attention now to a situation the details of which are much less understood from either a practical or theoretical standpoint than are chimney plumes, but which is of very considerable practical importance. This concerns the continuous discharge of buoyant material into rivers and/or estuaries, either from the bottom or at the shore. The best known discharge of this kind is hot water which has passed through the cooling system of power plants, etc. Merriman[13] has estimated that by the year 2000, 600 billion gallons of water per day will be required for cooling power plants or 50% of the average daily run-off in the United States. Such discharges occurring in streams of limited extent may lead to a variety of effects which have been generally described as thermal pollution.

The specific situation we wish to consider is illustrated in Fig. 6, and concerns the spreading out of the buoyant plume

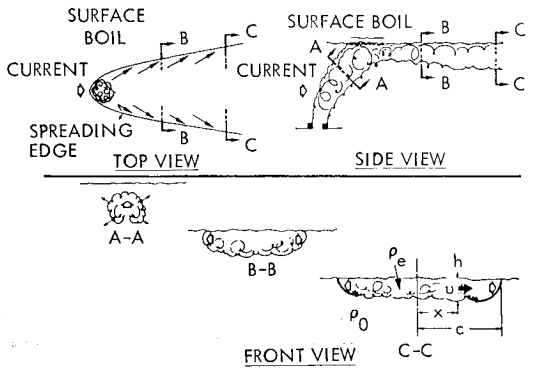

Fig. 6 Schematic of spreading buoyant discharge.

just beneath the free surface of the moving stream. We consider that the stream has bent over the plume and that it has impinged on the stream surface and has already begun to spread laterally. We would like to understand how this spreading occurs and is influenced by the various factors involved, particularly turbulent entrainment. We would particularly like to estimate how the temperature is diluted with distance downstream. The present work represents an attempt to analyze the fluid mechanics of the spreading process before the motions decay to the point where the stream turbulence itself governs the dispersion of the discharge.

In the theory which follows we take into account the gravimetric, inertial, and certain drag forces acting on the spreading mass. Entrainment into the mass is considered to arise from three possible sources: breaking of the head which exists at the edge of the spreading fluid; turbulence initially present in the spreading fluid and which decays with time; and turbulence continuously generated in the spreading fluid due to the action of wind shear. We will finally consider the asymptotic behavior of the spreading mass and show, in particular, how the decay of the excess temperature depends on the various entrainment processes considered.

Slender Body Approximation

We again appeal to the slender body approximation which proved so useful in the analysis of chimney plumes, but in this case we may take advantage of the additional circumstance that the spreading plume is much wider in the transverse section than it is thick. We thus neglect vertical velocities in comparison to the horizontal, and we characterize the flow at any horizontal distance from the centerline by values averaged over the vertical dimension.

We further assume that the exterior flow is in static equilibrium, an assumption which would seem to be valid except possibly in the immediate vicinity of the edge or head of the spreading mass.

The Head Flow

It has at various times been noted in connection with density currents and spreading oil films, that a bulge or arrow head formation develops at the head, often accompanied by vigorous mixing or breaking just behind the bulge. Indeed, as noted by Benjamin,[14] a steady density current must involve breaking and dissipation in order to balance the thrust which arises because of the hydrostatic pressures acting on the moving fluid. The argument may be summarized as follows. Since the flow is presumed steady and friction is neglected, the sum of hydrostatic and dynamic pressures acting on the fluid must vanish. The sum of hydrostatic pressures comprise a thrust of magnitude $(\Delta\rho)gh^2(o)/2$, see Fig. 7, where $h(o)$ is the thickness of the density current very far from the head and presumed uniform thereafter. It is well known that the sum of the dynamic pressures acting on a half-body (such as the density current assumed) is null. It therefore follows that the hydrostatic thrust must be balanced by a loss of pressure on the rearward facing part of the fluid body, such as accompanies mixing or breaking. (The situation is somewhat analogous to that at the rear of constant pressure cavities.) The net drag accompanying this loss of pressure must also be of magnitude $(\Delta\rho)gh^2(0)/2$. Should the external fluid involved in the mixing be incorporated into the density current and move with it, then a simple momentum balance shows that the increase in thickness of the density current is given by:

$$\delta^*/h(o) = \Delta\rho gh(o)/2\rho_e U^2 = 1/2F^2 \tag{19}$$

where δ^* is the displacement thickness of the wake due to breaking, ρ_e is the density of the exterior fluid,

$$F = U_o/\{(\Delta\rho)g[h(o)]\}^{1/2}$$

and U_o is the steady speed of the current. Since F is 0(1), according to experiment, it is clear that the steady entrainment implied by Eq. (19) is substantial. It is

$$dV/dt/h(o)U = \delta^*U/h(o)U = 1/2F^2 \tag{20}$$

where V is the volume of the current.

In the case of unsteady flow as is under consideration here, the above analysis is insufficient, for the net acceleration (or deceleration) of the spreading mass enters into the balance of forces. It is to be noted that a head drag of magnitude larger than the hydrostatic thrust will lead to a net deceleration of the spreading mass. Such a possibility must be contemplated since it would follow from the likely requirement that the speed of the head wave be Froude scaled (i.e., $u \infty (\Delta\rho gh/\rho)^{1/2}$, as is the limiting speed of disturbances in shallow water.

Entrainment and the Effect of Initial Turbulence

It is very likely that the existence of head drag is accompanied by significant entrainment as suggested above, and this possibility must be allowed in the analysis; very likely, too, the head entrainment and drag coefficients are proportional to one another. In the case of steady flow the latter is twice the former.

When the spreading mass originates through impingement as in the case of bottom discharge, it may be entraining all over its boundary due to the turbulent motion in its interior. This motion may be assumed to decay with time, neglecting the possible but presumably small regenerative effects due to shear at the boundary of the spreading mass, and within the breaker at the head (that is, we are particularly interested in the case where the initial turbulence intensity is large).

Further, if the water surface upon which the mass is spreading is subjected to sufficiently high wind shear, then turbulence within the mass will be continuously generated, and may cause entrainment at a rate which does not decay with time. All three entrainment possibilities mentioned in the preceding paragraphs will be considered.

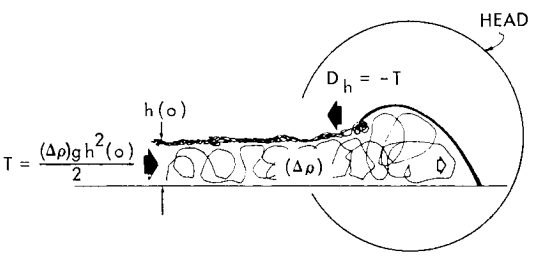

Fig. 7 Schematic of steady density current.

Conservation Laws

Excess Mass

The excess of the spreading fluid, δm_1, is

$$2\int_0^c (\rho_e - \rho_o)h dx = \delta m_1 \tag{21}$$

and upon the assumption that none of the fluid originally within the spreading mass is lost to the outer-fluid, then δm_1 is constant during the motion.

Volume

At the same time, the volume of the spreading mass does increase in time due to entrainment [except when the latter is absent, in which case $(\Delta\rho)$ is conserved]. Keeping in mind the discussion of the preceding section, we may calculate the volume increase:

$$\frac{d}{dt}\int_0^c h dx = \int_0^c Bv' dx + B'u(c)\cdot h \tag{22}$$

where B is the entrainment coefficient associated with the turbulence distributed within the spreading mass, whether due to original causes or maintained by wind shear, and B' is the head entrainment coefficient; v' is the turbulence intensity and $u(c)$ is the speed of the head.

Momentum Balance

Considering half of the spreading mass, its horizontal momentum must change at a rate equal to the difference between the hydrostatic thrust and the head drag:

$$\frac{d}{dt}\int_0^c \rho u h dx = \frac{(\Delta\rho)gh^2}{2} - D_h$$

$$\frac{d}{dt}\int_0^c \rho u h dx = \frac{(\Delta\rho)gh^2}{2}\bigg|_{x=0} - \frac{1}{2}\rho u^2(c)\cdot h(c)\cdot C_D' \tag{23}$$

We have neglected the friction between the inner and outer fluids acting along the fluid boundary, since it is small.

Turbulence Decay

Finally, as discussed earlier, we assume that the initial turbulence decays due to inertial turbulent interactions and without regeneration

$$\frac{d}{dt}\left\{\int_0^c \frac{3}{2}\rho v'^2 h dx\right\} = -\int_0^c C_D \frac{\rho v'^3 h dx}{h} \tag{24}$$

where we have assumed that the energy containing eddy scale is h, and where $C_D = 0(1)$. In the case of wind maintained turbulence, Eq. (24) is extraneous since $v' =$ constant. These Eqs. (21–24) cannot be readily considered without making additional simplifying assumptions, as we proceed to do below.

Similarity

We assume that, as often happens in turbulent flows (wakes and jets, for instance), the flow is self-similar in time, so that it may be characterized at any instant by characteristic quantities h^*, u^*, v^*, $\Delta\rho^*$, all functions of time. So

$$\begin{aligned} u(x,y,t) &= u^*(t/t_o)\cdot\bar{u}(x/c;\ y/h) \\ h(x,t) &= h^*(t/t_o)\cdot\bar{h}(\eta) \quad (x/c = \eta) \\ \Delta\rho(x,y,t) &= \Delta\rho^*(t/t_o)\cdot\Delta\bar{\rho}(\eta,\bar{y}) \quad (y/h = \bar{y}) \\ v'(x,y,t) &= v^*(t/t_o)\cdot\bar{v}(\eta,\bar{y}) \end{aligned} \tag{25}$$

The time t_o may be taken as h_o/u_o, where the latter are scales characterizing the initial conditions of the motion. We also require the barred quantities to be of order unity by taking:

$$\begin{aligned} u^* &= dc/dt \\ \int_0^1 \bar{h}(\eta)d\eta &= 1 \\ \int_0^1 \Delta\bar{\rho}(\eta)d\eta &= 1 \\ \int_0^1 \bar{v}(\eta)d\eta &= 1 \end{aligned} \tag{26}$$

Differential Equations for the Characteristic Quantities

Excess Mass, Eq. (21):

$$c\Delta\rho^* h^* = \frac{\delta m_1}{2}\left[\int_0^1 \Delta\bar{\rho}\bar{h}d\eta\right]^{-1} = \frac{\delta m_1}{2a_1} \tag{27}$$

where

$$a_1 = \int_0^1 \Delta\bar{\rho}\bar{h}d\eta$$

Volume, Eq. (22):

$$d/dt(ch^*) = v^* cB + u^* h^*[\bar{h}(c)\cdot B'] \tag{28}$$

Momentum, Eq. (23):

$$a_2 d/dt(u^* ch^*) = g(\Delta\rho^*/2\rho_o)h^{*2}\cdot a_3 - \tfrac{1}{2}u^{*2}h^*[\bar{h}(c)\cdot C_D'] \tag{29}$$

where

$$a_2 = \int_0^1 \bar{u}\bar{h}d\eta; \quad a_3 = (\Delta\bar{\rho}\bar{h}^2)_{x=0}$$

Eliminating $(\Delta\rho)^*$ by making use of Eq. (27), Eq. (29) becomes:

$$\frac{d}{dt}(u^* ch^*) = \left[\frac{g\delta m_1\cdot a_3}{4a_1\rho_o a_2}\right]\frac{h^*}{c} - \frac{u^{*2}h^*}{2}\cdot\left[\frac{\bar{h}(c)C_D'}{a_2}\right] \tag{30}$$

Turbulent Energy, Eq. (24):

$$d/dt(cv^{*2}h^*) = -v^{*3}c[(2C_D\cdot a_4)/3] \tag{31}$$

where

$$a_4 = \left(\int_0^1 \bar{v}^3 d\eta\right)\Big/\left(\int_0^1 \bar{v}^2\bar{h}d\eta\right)$$

The simultaneous solution of Eqs. (28, 30, and 31) leads to a specification for $c(t)$, $v^*(t)$, and $h^*(t)$. The solutions depend, of course, upon the parameters B, B', C_D, and C_D', all of which we estimate to be 0(1). Inspection of the governing equations shows that the motions are likely to be quite different when in their early and late stages.

Power Law (Asymptotic) Variation of the Characteristic Quantities

Under certain conditions it is possible to find power law variations for the characteristic quantities:

$$\begin{aligned} u^* &= u_o(t/t_o)^\alpha \text{ or } c = [u_o t_o/(\alpha+1)]\,(t/t_o)^{\alpha+1} \\ h^* &= h_o(t/t_o)^\beta \\ \Delta\rho^* &= (\Delta\rho)_o(t/t_o)^\gamma \\ v^* &= v_o(t/t_o)^\delta \end{aligned} \tag{32}$$

In the present work we restrict our attention to these cases which certainly refer to the late stages of the motion. We shall be able to estimate the influence of initial conditions, mixing, and dissipation upon the exponents α, β, γ, and δ and in this way to speculate about the asymptotic spreading and dilution which occurs naturally under the influence of various initial conditions.

The substitution of Eq. (32) in Eqs. (27–31) leads to

$$\left(\frac{t}{t_o}\right)^{\alpha+\beta+\gamma+1} = \frac{(\alpha+1)}{2a_1}\frac{\delta m_1}{h_o u_o t_o (\Delta\rho)_o} \tag{33}$$

$$(\alpha+\beta+1)\left(\frac{t}{t_o}\right)^{\alpha+\beta} = B\cdot\frac{v_o}{u_o}\left(\frac{t}{t_o}\right)^{\alpha+\delta+1} + [B'\bar{h}(c)](\alpha+1)\left(\frac{t}{t_o}\right)^{\alpha+\beta} \tag{34}$$

$$(2\alpha+\beta+1)\left(\frac{t}{t_o}\right)^{2\alpha+\beta} = \left[\frac{g(\Delta\rho)_o}{\rho_o}\frac{h_o}{u_o^2}\right]\left[\frac{a_3}{2a_2}\right]\times (4+1)\left(\frac{t}{t_o}\right)^{\beta-\alpha-1} - \left[\frac{\bar{h}(c)C_D'}{a_2}\right]\frac{(\alpha+1)}{2}\left(\frac{t}{t_o}\right)^{2\alpha+\beta} \tag{35}$$

$$(\alpha+\beta+1+2\delta)\left(\frac{t}{t_o}\right)^{\alpha+\beta+2\delta} = -\left[\frac{2C_D a_4}{3}\right]\frac{v_o}{u_o}\left(\frac{t}{t_o}\right)^{3\delta+\alpha+1} \tag{36}$$

The assumed laws of variation are only possible if each term in any given equation above is of the same degree in t. As a result it is necessary that:
From Eq. (35)

$$\alpha = -\tfrac{1}{3} \tag{37}$$

Eqs. (33) and (37)

$$-\gamma = \beta + \tfrac{2}{3} \tag{38}$$

Eqs. (34) and (36)

$$\delta = \beta - 1 \tag{39}$$

These relations while clearly not sufficient by themselves (they do not lead to a determination of β, γ, or δ), nevertheless reveal a great deal about possible motions.

First of all, they show the invariance of the head Froude number, which is proportional to the following quantity:

$$F^* = \frac{u^*}{[(\Delta\rho)^* g h^*]^{1/2}} = \frac{u_o}{[(\Delta\rho)_o g h_o]^{1/2}}\left(\frac{t}{t_o}\right)^{\alpha-\gamma/2-\beta/2} = \frac{u_o}{[(\Delta\rho)_o g h_o]^{1/2}}, \text{ a constant} \tag{40}$$

according to Eqs. (38) and (39). Second, they show that the width of the spreading mass follows the same asymptotic law, independent of the entrainment mechanism,

$$c \sim (t/t_o)^{2/3} \tag{41}$$

Third, the laws of motion immediately follow in the case where the entrainment is due to head entrainment plus a constant level of turbulence maintained by wind shear. In this case $\delta = 0$ so that

$$\alpha = -\tfrac{1}{3} \quad \beta = +1 \quad \gamma = -\tfrac{5}{3} \tag{42}$$

We note in this case that the vertical spreading rate will eventually exceed the horizontal.

Finally, it is possible to calculate the requirement for the maintenance of a continuous balance between turbulent and gravimetric effects. These are (a turbulent Froude number) in the ratio,

$$\frac{v^{*2}}{(\Delta\rho)^* g h^*} = \frac{v_o^2}{(\Delta\rho)_o g h_o}\left(\frac{t}{t_o}\right)^{2\delta-\gamma-\beta} = \frac{v_o^2}{(\Delta\rho)_o g h_o}\left(\frac{t}{t_o}\right)^{2\beta-4/3} \tag{43}$$

and declines with time unless $\beta > \frac{2}{3}$. This is also the condition that the vertical and horizontal spreading rates are in constant proportion. We have already seen that $\beta = +1$ if turbulence is maintained externally as by the wind so that in this case the stability to turbulence mixing of the zone between the spreading fluid and the outer stream actually decreases with time, thus aiding in the maintenance of rapid vertical spreading. We shall later see that in the absence of maintained turbulence, $\beta < \frac{2}{3}$, so that the turbulent Froude number declines rather than increases. As a result, entrainment due to decaying initial turbulence will eventually be severely inhibited.

Now in addition to Eqs. (37–39), the cancellation of the time dependence in Eqs. (33–36) leaves the following relations which must be satisfied:

$$\delta m_1 = 2a_1 h_o u_o t_o (\Delta\rho)_o/\alpha + 1 = 3a_1(\Delta\rho)_o h_o^2 \tag{44}$$

which provides a definition of h_o.

$$(\beta + \tfrac{2}{3}) = B(v_o/u_o) + \tfrac{2}{3}[B'\bar{h}(c)] \tag{45}$$

$$(\beta + \tfrac{1}{3}) = (a_3/3a_2)\cdot F_o^{-2} - \{[\bar{h}(c)\cdot C_D']/3a_2\} \tag{46}$$

$$(3\beta - \tfrac{4}{3}) = -(2C_D a_4/3)(v_o/u_o) \tag{47}$$

The constants B, B', C_D, C_D', a_2, a_3, a_4, and $\bar{h}(c)$ being fixed these have a solution only for specific values of v_o/u_o and F_o.

We present below illustrative calculations for the three separate cases of interest: 1) no initial or maintained turbulence; 2) initial turbulence which decays with time; and 3) maintained turbulence. Taking $C_D'/a_2 = 2B'$; $a_3/a_2 = 1$; $B = \frac{1}{2}$; $a_4 C_D = 1$, Table 1 results.

These calculations show that the change of thickness of the spreading mass with time is particularly sensitive to the existence of turbulence, and so in turn is the rate at which dilution occurs.

Comparison with Observations

There seems to exist no systematic laboratory investigations of the kind of spreading flow under discussion here, and only limited full-scale observations, notably those of Foxworthy, Tibby, and Barsom.[15] Some correlation may be made however, between the theory and the data which are available.

Sharp Edge

In the theory presented here, transverse spreading is due to and is governed by gravimetric pressures, resulting in a head flow at constant Froude number. At least the notion of such a flow, resulting in a sharp edge or separation between the spreading mass and the surrounding fluid is very well substantiated by aerial photographs of spreading discharge as in Foxworthy et al. (1966).[15] The sharp and continuous edges which are evident in such photographs offer

Table 1 Parameters pertaining to asymptotic spreading

Case	$B'\bar{h}(c)$	v_o/u_o	F_o^2	α	β	γ	δ
(1)	$\frac{1}{2}$	0	1	$-\frac{1}{3}$	$-\frac{1}{3}$	$-\frac{1}{3}$	...
	1	0	$\frac{1}{3}$	$-\frac{1}{3}$	0	$-\frac{2}{3}$	...
(2)	$\frac{1}{2}$	$\frac{16}{13}$	$\frac{5}{13}$	$-\frac{1}{3}$	$\approx\frac{1}{5}$	≈ -0.9	≈ -0.8
	1	$\frac{8}{13}$	$\frac{5}{18}$	$-\frac{1}{3}$	$\frac{4}{13}$	≈ -1.0	≈ -0.7
(3)	$\frac{1}{2}$	$\frac{8}{3}$	$\frac{1}{5}$	$-\frac{1}{3}$	$+1$	$-\frac{5}{3}$	0
	1	2	$\frac{1}{6}$	$-\frac{1}{3}$	$+1$	$-\frac{5}{3}$	0

clear evidence that transverse spreading is a non-random process and is therefore not due to turbulent dispersion.

Spreading and Dilution

Foxworthy, et al.[15] observed the near-surface spreading of a large (72 in. diam; 340,000 m^3/day) sewage outfall discharge into the sea at a depth of 50 ft. The waste mixture rises to the surface, forms a large turbulent boil and then moves away from the boil area in the direction of the prevailing surface current. The investigators measured the downstream concentration of dye which they had injected near the boil; they reported laws of dye concentration decay with downstream distance, and laws for the growth of the transverse and vertical dispersion of the spreading dye. They were able, in almost all cases, to fit their observations of spreading and dilution with power laws, so that their exponents may be directly compared with the results of our theory.

They have given laws for lateral dispersion in 6 cases, their experiments 1, 2, 4, 6, 7, and 9. From these, laws of variation of width with downstream distance may be deduced, corresponding to $c \sim x^{0.78}$, which may be compared to the theoretical prediction $c \sim x^{2/3}$.

In all of their experiments, a wind was reported rising during the day. The reported average wind speed varied between 1.6 and 7.6 knots. We will consider their reported laws of dilution and of vertical spreading separately for the case with the lowest wind speed and for all the rest combined in Table 2.

Table 2 Observed spreading parameters

Wind Speed	β (obs.)	γ (obs.)
1.6 knots (3.3–7.6 knots)	0.1	−0.98
5.7 knots average	0.56	−1.51

The low wind speed result for dilution seems to be in good agreement with the predictions made for the case of initial but decaying turbulence, although the observed vertical spreading seems somewhat less pronounced than predicted in this case, see Table 1. For the higher wind speeds, the increase in dilution decay is marked, but not to the extent predicted by the theory assuming maintained turbulence ($\gamma = -\frac{5}{3}$); at the same time, the vertical spreading was also more marked than at the low wind speed, but was not as pronounced as theory predicts ($\beta = +1$). These data certainly serve to show up the importance of wind-induced mixing. It would naturally be highly desirable to make further comparisons between theory and systematic data, especially as may be acquired under controlled laboratory conditions.

References

[1] Keffer, J. F. and Baines, W. A., "The Round Turbulent Jet in a Cross Wind," *Journal of Fluid Mechanics*, 1963, Vol. 15, pp. 481–496.

[2] Keffer, J. F., *The Physical Nature of the Subsonic Jet in a Cross-Stream*, NASA SP-218, 1969, pp. 19–36.

[3] Scorer, R. S., *Natural Aerodynamics*, Pergamon Press, New York, 1958.

[4] Hoult, D. P., Fay, J. A., and Forney, L. J., "A Theory of Plume Rise Compared with Field Observations," Paper 68-77, 1968, Air Pollution Control Association, Pittsburgh, Pa.

[5] Shwartz, J. and Tulin, M. P., "Chimney Trails in a Stratified Atmosphere," *Proceedings of the 2nd Annual North Eastern Regional Antipollution Conference*, University of Rhode Island, 1969.

[6] Morton, B. R., Taylor, G. I., and Turner, I. S., "Turbulent Gravitational Convection from Maintained and Instantaneous Sources," *Proceedings of the Royal Society*, A23, 1956, pp. 1–23.

[7] Tulin, M. P. and Shwartz, J., "The Motion of Turbulent Vortex Pairs in Homogeneous and Density Stratified Media," *Proceedings of the 8th ONR Symposium on Naval Hydrodynamics*, California Institute of Technology, 1970.

[8] Briggs, G. A., "A Plume Rise Model Compared with Observations," *Journal of the Air Pollution Control Association*, Vol. 15, 1965, pp. 433–438.

[9] Slawson, P. R. and Csanady, G. T., "On the Mean Path of Buoyant Bent-Over Chimney Plumes," *Journal of Fluid Mechanics*, Vol. 28, 1967, pp. 311–322.

[10] Bringfelt, B., "Plume Rise Measurements at Industrial Chimneys," *Atmospheric Environment*, Vol. 2, 1968, pp. 575–598.

[11] Wu, J., "Mixed Region Collapse with Internal Wave Generation in a Density Stratified Medium," *Journal of Fluid Mechanics*, Vol. 35, 1969.

[12] Tsang, G., "Concentration of Effluents in a Plume as Predicted by a Model and Observed in Field," Fluid Mechanics Laboratory Publication 69-7, Dept. of Mechanical Engineering, MIT, Cambridge, Mass.

[13] Merriman, D., "The Calefaction of a River," *Scientific American*, Vol. 222, No. 5, May 1970, pp. 42–61.

[14] Benjamin, T. B., "Gravity Currents and Related Phenomena," *Journal of Fluid Mechanics*, Vol. 31, 1968, pp. 209–248.

[15] Foxworthy, J. E., Tibby, R. B., and Barsom, G. M., "Dispersion of a Surface Waste Field in the Sea," *Journal of the Water Pollution Control Federation*, Vol. 38, No. 7, July, pp. 1170–1193.